HHS Public Access

Author manuscript

IEEE Access. Author manuscript; available in PMC 2017 February 28.

Published in final edited form as:

IEEE Access. 2016 ; 4: 893–904. doi:10.1109/ACCESS.2016.2535661.

A Perturbation Mechanism for Investigations of Phase-Dependent Behavior in Human Locomotion

Dario J. Villarreal [Student Member, IEEE],
Department of Bioengineering, University of Texas at Dallas, Richardson, TX 75080, USA

David Quintero [Student Member, IEEE], and
Department of Mechanical Engineering, University of Texas at Dallas, Richardson, TX 75080, USA

Robert D. Gregg [Member, IEEE]
Departments of Bioengineering and Mechanical Engineering, University of Texas at Dallas, Richardson, TX 75080, USA

Dario J. Villarreal: dario.villarreal@utdallas.edu; Robert D. Gregg: rgregg@ieee.org

Abstract

Bipedal locomotion is a popular area of study across multiple fields (e.g., biomechanics, neuroscience and robotics). Different hypotheses and models have tried explaining how humans achieve stable locomotion. Perturbations that produce shifts in the nominal periodic orbit of the joint kinematics during locomotion could inform about the manner in which the human neuromechanics represent the phase of gait. Ideally, this type of perturbation would modify the progression of the human subject through the gait cycle without deviating from the nominal kinematic orbits of the leg joints. However, there is a lack of publicly available experimental data with this type of perturbation. This paper presents the design and validation of a perturbation mechanism and an experimental protocol capable of producing phase-shifting perturbations of the gait cycle. The effects of this type of perturbation on the gait cycle are statistically quantified and analyzed in order to show that a clean phase shift in the gait cycle was achieved. The data collected during these experiments will be publicly available for the scientific community to test different hypotheses and models of human locomotion.

Index Terms

gait analysis; perturbations; locomotion control; phase-dependent behavior

I. INTRODUCTION

BIPEDAL locomotion is a trademark of humans and few other species on this planet. Understanding the control principles on how bipedal locomotion works as well as the biological processes involved has been a popular subject of study. As a consequence, different hypotheses on the evolutionary history as well as on the functional behavior of walking have been investigated [1]. The benefits of studying and understanding human locomotion can be transcendental by, for example, helping design powered prosthetic legs that could mimic the behavior of natural limbs. This would allow amputees to walk more

naturally and efficiently. Understanding how humans react to external perturbations while walking (e.g., tripping, slipping, etc.) is also of importance as it can be meaningful to multiple applications (e.g., prevention of falls in older populations [2], [3], safety in industry [4], prosthetic design and control [5], [6], and bipedal robots [7]–[11]).

Different hypotheses and models explaining how the human body is able to achieve stable locomotion have been previously proposed. These hypotheses and models agree that the human body needs to somehow synchronize the leg joints in order to achieve stable walking. Some hypotheses have proposed that there exists an internal clock, such as a central pattern generator (CPG) [12]–[14] or coupled oscillators [15], [16], helping keep the body synchronized and in rhythm through the entire gait cycle. However, other hypotheses propose that synchronization during walking could be achieved merely by reflex responses and that only synergistic cooperation between proprioception feedback and muscle activation is necessary to achieve stable locomotion [17]. These models inform neuroscientists about the different neural architectures that might be used in humans during locomotion. These models have been extensively studied in computer simulations [17], [18], but it would be of great interest to the scientific community to use human data to validate their accuracy.

A key feature describing the synchrony of multi-joint patterns is the phase of gait. In a periodic process, such as the gait cycle, phase is a scalar quantity representing the location on the periodic orbit of multi-joint kinematics. Specifically, if this quantity is given at a particular point in time then it is possible to determine the entire configuration of the system along the nominal periodic orbit. Due to the complexity and the vast amount of degrees of freedom involved in locomotion, it is difficult to compute and sketch a multidimensional representation of the gait cycle’s phase. The previously mentioned neuromechanical hypotheses have different ways of representing the phase of the gait cycle (i.e., the overall synchronization of the leg joint patterns), often depending on the entire system state or extended states in higher-dimensional dynamics. To address this challenge, it has been proposed that a single mechanical variable could provide a robust representation of gait cycle phase [6], [19]. Perturbation experiments capable of shifting the timing of the gait cycle would be useful to validate the efficacy of these different models and hypotheses at representing phase in human locomotion.

Perturbation experiments are used to understand and study the underlying principles governing the behavior of a system (in our case the gait cycle) [20]. In particular, one can determine specific properties of the biomechanics governing the gait cycle by analyzing a human subject’s response after a perturbation (e.g., [21]–[24]). For this methodology it becomes obvious that the perturbation itself needs to be controlled, repeatable, and unexpected to the subject in order to reliably identify the natural human response. To study inter-joint synchronization, these perturbations should occur along the nominal periodic orbit of the system in order to elicit a phase-shifting response rather than transient corrections back to the nominal orbit.

A data set of the human response to phase-shifting perturbations is needed in order to test the different hypotheses on the neuromechanics of the human gait cycle. In particular, the

literature lacks publicly available data about the human response to multi-joint phase-shifting perturbations in order to correctly validate the different neuromechanics hypotheses. We propose that translational anterior-posterior perturbations of the stance foot will accelerate or decelerate the progression of the gait cycle without substantially deviating from the nominal period orbit of the leg joints. This kinematic response could then be used to compare and validate the current results gathered from computer simulations of the different hypotheses. This paper presents the design of a mechanism paired with an experimental protocol capable of producing phase-shifting perturbations of the gait cycle. We validate the mechanism and protocol design by showing that a phase shift occurs along the nominal periodic orbit of the leg joint kinematics.

A. Related Work

Perturbing the gait cycle is one of the most common methods used to study properties associated with the response of the human body during locomotion. Perturbation studies often consist of unexpectedly disturbing one or more leg joints during walking, thus disrupting specific periods of the gait cycle. There are different biomechanical properties that can be studied from such experiments (e.g., joint impedances [21]–[25], gait cycle phase [6], [26], etc.). The type of perturbation used in a particular experiment is highly dependent on the biomechanical property that needs to be studied.

As an example, if the impedance of a particular joint is to be studied experimentally then joint-level perturbations are carefully designed for the joint [22]–[25]. However, if a hypothesis regarding the overall gait cycle is being studied (e.g., behavior of humans to slipping conditions), then a multi-joint perturbation might be needed [3], [4], [27], [28]. In this paper we focus mainly on multi-joint perturbations since we are looking at phasing of the gait cycle rather than the behavior of a specific joint.

Examples of mechanisms capable of producing multi-joint perturbations can be found in [3], [4], [19], [27]–[30], where different hypotheses and properties were studied. In [30] the response of people to slipping conditions was studied, whereas in [27] a multi-axial machine was specifically built and validated to alter the gait cycle in different directions. These papers did not focus on producing a phase shift along (or tangential to) the nominal orbit of the gait cycle. In addition, the data sets of these experiments are not publicly available and thus cannot be used to study different hypotheses. In the case of slip studies [3], [4], the perturbations are not bidirectional at specific phases and thus cannot study forward and backward phase shifts. Moreover, the displacement of the center of mass (COM) and onset time of the perturbation cannot be controlled in a slip. One exception is the controlled slip allowed by the mechatronic shoe in [31], [32]. In this paper we focus mainly on perturbations capable of producing a phase shift of the gait cycle in a controlled, repeatable manner.

Phase-shifting perturbations can be produced by mechanically manipulating the leg joints [19] or by changing the sensory perception of a subject walking [33]. A phase-shifting perturbation slows or advances the overall progression of the gait cycle (i.e., decelerating or accelerating through the leg joint patterns). Ideally for studying inter-joint or inter-limb synchronization, a clean phase shift would not disrupt the periodic orbits of the joints, thus

keeping them synchronized at a different location on the orbit. Previous experiments studying mechanical phase perturbations were done using rotational perturbations occurring only at the ankle in [26]. The difference between these previous experiments and ours is that we are evoking an overall gait (i.e., multi-joint) response. The main goal in this paper is to provide the design of a machine capable of producing perturbations as well as an experimental protocol to study phase-dependent control mechanisms of human locomotion.

A preliminary design of the mechanism and experimental protocol can be found in [19]. In the present study, the results of only one able-bodied subject were used to demonstrate the ability of a mechanical variable to represent the phase of gait. In this paper, we give a more detailed explanation of the experimental protocol, present data for ten human subjects, and statistically show the phase-shifting effects of the perturbation on the human subjects' gait cycle.

B. Contribution

Experimental data is necessary to validate different models and hypotheses related to the neuromechanics involved in the gait cycle (e.g., CPG, neuroreflex models, etc.). Each of these models has been extensively studied using computer simulations, but there is a lack of experimental data to validate the ability of such models to represent gait cycle phasing. We propose an experimental protocol, in conjunction with the design of a custom machine capable of producing phase-shifting perturbations, to collect quantitative data for the study of such models and hypotheses. The data gathered from these experiments will be publicly available to researchers. We envision that this data will be a powerful tool, when combined with modeling and simulation results, in understanding the different hypotheses describing human locomotor control.

In addition to the study of different neuromechanical models, the data from these experiments can help in the investigation of biomechanical properties of the human leg. For example, these experiments can be used to validate the hypothesis of a single mechanical variable as a robust representation of the phase of the gait cycle (i.e., the phase variable hypothesis) [6]. How humans control their interlimb coordination during the gait cycle is another question that can be studied with the data from these experiments. In particular, one could answer the question of how humans synchronize their leg patterns after a phase-shifting perturbation to only one leg [6]. Overall, these experiments can inform researchers about the human response to step input perturbations.

The experimental protocol designed in this paper targets the human responses to phase-shifting perturbations. The protocol was validated through statistically comparing the gait cycle's time shift produced by different perturbation timings and directions as well as the similarity (i.e., correlation coefficient) between perturbed and non-perturbed joint trajectories. These metrics prove that the perturbations produced clean phase shifts in the gait cycle. The neuromuscular response of the human subjects to the experiment was analyzed by comparing abnormal co-contractions of several leg muscle groups. Section II presents the design of the mechanism and validates its ability to produce quick perturbations under loads. Section III explains the experimental design and statistical analyses conducted

to validate the phase shifting perturbations across ten able-bodied subjects. Finally, in Section IV the behavior of human subjects to phase shifting perturbations is discussed.

II. DESIGN AND VALIDATION OF THE PERTURBATION MECHANISM

In this section the electromechanical design of the perturbation mechanism will be reviewed. The hardware and software integration that allowed data collection and control of the mechanism during the experimental procedure will be discussed. This section finally presents experimental results to validate the design of the mechanism (e.g., trajectory and forces of the perturbation).

A. Design

The mechanism was designed to perturb the progression of the gait cycle in a uniaxial direction (i.e., anterior-posterior direction). This axis was chosen because the progression of the gait cycle is correlated with the anterior-posterior position of the body's COM with respect to the stance foot. In other words, moving the stance foot forward or backwards during the gait cycle should effect a phase shift.

The perturbations elicited by the machine needed to be as fast as possible in order to produce an almost instantaneous kinematic phase change in the gait cycle of the subject. The perturbation duration was chosen to be approximately 100 ms. In order to avoid a trip response, the magnitude of the perturbation (i.e., total linear displacement of the mechanism) needed to be within a specific range to modify steady gait without interrupting the gait cycle (i.e., without deviating the leg joint angles outside their nominal range of motion). Mathematically this type of perturbation could keep the dynamical state of the human on or nearby the nominal periodic orbit but with a shift in phase (or location along the orbit). Even though there have been experiments perturbing the gait cycle using a treadmill [34]–[36], our mechanism was design to provide faster perturbations that those achievable on a treadmill.

The largest perturbation considered for this purpose would cause a 5 degree change in the global leg angle (the angle between vertical and the vector going from the hip joint to the ankle), which normally has a 60 degree range of motion [37]. Assuming the hip position remains stationary during the perturbation, a 10 cm displacement would cause approximately a 5 degree change in the global leg angle. Although the mechanism was designed for this maximum displacement, our human subjects study only considered 5 cm perturbations for safety reasons. The values of the acceleration and speed necessary for the perturbation were calculated using a linear segment with parabolic blends (LSPB) method, where the constraints enforced were the specific displacement and time duration for the perturbation.

These perturbations needed to be produced in both the forward and backward directions (i.e., in and against the direction of walking, respectively, as shown in Figure 2) to induce both forward and backward phase shifts and to prevent subjects from compensating for anticipated perturbations in any one direction. The mechanism was also designed to

withstand normal impact loads of up to 240 kg, since future experiments may involve subjects running.

A rod-style ball nut screw drive linear actuator (Model: SPL-RSA50-BN01-SK9-LMI-MP2-CLV, Tolomatic, Inc., Hamel, MN, USA) was used to move the force plate (i.e., contact surface) horizontally on top of the mechanism, Figure 1. This actuation system was custom made to achieve the specified displacement, speed, and loading requirements. The actuator was set in motion by a 2 kW AC servomotor (Model: R2AA13200DXP00M, SANYO DENKI CO., LTD., Tokyo, Japan). The motor was mounted in-line with the linear actuator to give a direct drive actuation. This yielded a faster and more efficient mechanism. The motor required a 3 phase, 220 VAC power input and was fused at 20 A. The rated torque of the motor was 6.37 Nm. It was controlled by a servo amplifier (Model: RS1A10AA, SANYO DENKI CO., LTD., Tokyo, Japan) with closed-loop position control using an optical, high resolution absolute encoder (Model: PA035, SANYO DENKI CO., LTD., Tokyo, Japan). The control scheme was a PID controller, where the PID gains could be set for the motor to get a desired performance response for the actuation system. The combination of the servomotor and the rod-style actuator fulfilled the desired specifications.

A portable force plate (Model: 9260AA6, Kistler, Winterthur, Switzerland) was mounted onto an adapter plate on top of the actuator. When a subject stepped on the force plate, the mechanism would activate the motor after a predetermined time delay, thus setting the mechanism in motion. The adapter plate was guided by four linear load bearings through steel rails. These rails permitted only a horizontal motion of the adapter plate and the force plate, Figure 1. The end-effector of the actuator was attached to the center of the adapter plate from below. As a safety measure, the perturbation mechanism had two reed switches that could stop the actuator outside its specific range of motion.

In order to integrate the sensing and actuation instruments of the perturbation mechanism, a Programmable Logic Controller (PLC, Model: CTC5220, Control Technology Corporation, MA, USA) was used. The PLC had multiple analog and digital I/Os. The reed switches and the emergency stop button were connected to the digital inputs. Two channels of the force plate were connected to the analog inputs of the PLC and a threshold signal was set to detect contact with the force plate. The digital and analog outputs of the PLC were connected to the servo amplifier, allowing control of the servomotor. Low-level algorithms were programmed in the PLC to control different actions of the motor (see Section III-A). An external PC was used to oversee and direct these algorithms according to the experimental protocol described in the following section. The communication between the PLC and the computer was done using TCP/IP through an ethernet cable and an OPC server client. Figure 3 shows a general overview of the routing connections and hardware components.

B. Validation of the Mechanism

We tested the ability of the machine to provide fast step input perturbations. The machine was set at its maximum velocity ($v = 1\ m/s$) and an upper bound on the acceleration was chosen ($a = 100\ m/s^2$). Step inputs of several magnitudes were commanded to the machine, and the time to achieve such magnitudes was recorded (Δt). For each magnitude the step input was repeated ten times and the experimental time and magnitudes were measured and

averaged. Figure 4 shows the average time period (Δt) needed to achieve a specific magnitude. It can be seen that the mechanism is able to provide fast and high amplitude step input perturbations as needed to effect phase shifts to the gait cycle.

The perturbation mechanism was embedded in the middle of an 8 m walkway (Figure 2), where the top of the force plate was level with the walkway surface. The target perturbation profile (i.e., 5 cm in 100 ms) was validated with the mechanism under loaded and unloaded conditions (i.e., with and without a human subject stepping on it). A motion capture system (Vicon, Oxford, UK) was used to collect the motion of the mechanism by attaching reflective markers to the force plate (Figure 1). A total of 40 perturbations were commanded to the mechanism with no subject walking on top of the force plate (i.e., unloaded condition) and the mean perturbation motion was computed, Figure 5. It can be seen that the magnitude and response time of the perturbation correspond to the ideal perturbation (i.e., 5 cm in 100 ms). Later, a total of 40 perturbations were commanded to the mechanism when a person was stepping onto the force plate (i.e, loaded condition) during walking over an elevated walkway. The mean perturbation trajectories of the loaded and unloaded conditions can be seen in Figure 5, and both are almost identical in magnitude and response time. In fact, the correlation coefficient between these two perturbation trajectories is 0.99. This shows that the perturbation profile commanded was invariant to human loads on the mechanism.

C. Effects of Perturbations on the Force Plate

The effect of the high acceleration perturbations on the force plate resulted on unwanted high frequency noise, specifically in the direction of motion (the x-axis of the force plate). We computed the frequency response of the force plate channels, using a fast fourier transformation algorithm (FFT) in MATLAB, under loaded conditions (Figure 6). Noise is visible in the high frequency bands of the x-axis and not visible in the y- or z-axis of the force plate. We concluded that a low-pass second-order Butterworth filter with a cutoff frequency of 20 Hz (implemented in MATLAB) would be adequate to remove the majority of the noise from the force plate channels as in [21], [26]. The performance of the filter in the force channels can be seen in Figure 7.

III. DESIGN AND VALIDATION OF THE EXPERIMENTAL PROTOCOL

In this section we will review the experimental protocol intended to produce phase shifts in a human's gait cycle. We will present the experimental results and the statistical analysis that shows that the human subjects experienced a clean phase shift along the nominal periodic orbit of the leg joint kinematics.

A. Experimental Protocol

The experimental protocol was approved by the Institutional Review Board at the University of Texas at Dallas. A total of ten able-bodied subjects (4 women) were recruited in order to validate the experimental design and collect a sufficient data set for statistical tests of motor control hypotheses. The adult human subjects (Mean ± STD, height: 175.44 cm ± 6.10 cm, weight: 67.25 kg ± 7.40 kg) gave written informed consent of the experimental protocol prior to experimentation. Anthropomorphic measurements (e.g., leg length, hip width, knee

width, etc.) were taken from each subject and later entered into the motion capture software Nexus (Vicon, Oxford, UK) to create a 3D kinematic model with the help of the Plug-in-Gait module. Reflective markers and surface EMG sensors were placed onto the legs as described in Section III-B. Subjects were asked to wear comfortable clothes that would not interfere with motion capture.

The experiment contained four sets of 72 trials, where each trial consisted of the subject walking from a fixed starting point, stepping with their right foot on the force plate in the middle of the walkway, and continuing to walk until the end of the walkway, Figure 9. Although force plate targeting does not significantly alter gait kinetics [38] or kinematics [39], the subject was given time before data collection to find a preferred starting point on the walkway to achieve consistent, clean contact on the force plate with minimal targeting. Handrails were located along the walkway to mitigate the risk of falling, but the subjects did not use them at any time during the experiments.

The perturbation start time was chosen randomly as 100 ms, 250 ms, or 500 ms after initial contact (IC) with the force plate. At these specific times, the hip, knee, and ankle joints are typically in a monotonic region of the gait cycle. Thus, a perturbation at these instants would not cause the joints to deviate from their usual range of motion during steady gait and would keep the joint kinematics on the nominal periodic orbit to effect a clean phase shift. A supplemental video of these perturbation conditions is available for download.

The PLC initiated one of three preprogrammed subroutines whenever the subject stepped on the force plate (triggered by a vertical force of 25 N, Figure 8). The first option set the motor into an immobile state for no perturbation. The second and third options respectively set the mechanism into forward or backward motion—in or against the direction of walking—after a randomized delay of 100 ms, 250 ms, or 500 ms from IC. The force plate traveled a distance of 5 cm over 100 ms in either direction.

In order to decide what perturbation condition would occur, a randomized array of conditions was created using MATLAB (MathWorks, Natick, MA, USA). This array was configured to give non-perturbations a 50% probability of incidence, and the forward or backward conditions a 25% probability of incidence each. For the forward or backward conditions the perturbation timings were randomized with equal probability. This array was set into LabVIEW (National Instruments, Austin, TX, USA) to control the onset of each subroutine programmed in the PLC.

B. Data Acquisition

Besides serving as a triggering device, the force plate mounted on the perturbation mechanism was also used to collect the subject’s GRF at a sample rate of 1 kHz. The force plate measurements were filtered as described in Section II-C.

Kinematic data was collected by ten motion capture cameras (Model: T20S, Vicon, Oxford, UK) that measured the 3D spatial coordinates of reflective markers attached to bony landmarks on the subject’s body. The data acquisition rate for the cameras was set to 100 Hz. The hip, knee, and ankle joint angle kinematics were captured for both legs during the

experiment. A total of eight Trigno wireless surface EMG sensors (Delsys, Natick, MA) were attached to the subject's major muscle groups on their legs. Specifically, a sensor was placed in the vicinity of the rectus femoris (RF), biceps femoris (BF), tibialis anterior (TA), and gastrocnemius (GC) for each leg. All data collected from the force plate, EMG sensors, and cameras were synchronized through the use of a Giganet box (Vicon, Oxford, UK). This data was then stored in Vicon Nexus, which directly filtered and post-processed the kinematic data. Impulses in the force plate measurements and the velocity of the heel marker were used to define the gait cycle period.

The data was post-processed in a custom MATLAB script that detected outliers. The trials whose kinematic data (i.e., hip, knee, and ankle joint angles) were three standard deviations away from the mean were treated as outliers and thus removed from the overall pool of meaningful kinematic data. The EMG signals were rectified and low-pass filtered (second order bi-directional Butterworth low-pass filter, fc = 40 Hz). Outliers were removed, per subject, for trials where the EMG signal was three standard deviations away from the mean. The signals were normalized, per subject, with respect to the maximum contraction that occurred during the experiment (i.e., 4 sets of 72 trials, Section III-A). Finally, the average EMG signals were computed for each perturbation condition and subject [40].

C. Validation of the Experimental Protocol

The experimental protocol was conducted with a total of ten able-bodied subjects. A supplemental downloadable dataset contains the subject-specific means and standard deviations for the joint kinematics, ground reaction forces, EMG activations, and temporal gait parameters. This section analyzes the dataset in order to validate the experimental protocol and the dataset itself for use in studies of phase-dependent behavior.

The across subject average joint kinematics were obtained to verify that the perturbations shifted the gait cycle with respect to its original timing. Figure 11 shows the joint kinematics with perturbations occurring at 100 ms and 250 ms. For both onset times it can be seen that, in general, a forward perturbation (i.e., the mechanism moves the stance foot forward) decelerates the gait cycle and thus the gait cycle has a longer duration to completion. A backward perturbation accelerates the gait cycle and produces a shorter duration of gait cycle. This supports our protocol and mechanism design for affecting the phase of the gait cycle. The results for the onset time of 500 ms are omitted because those perturbations did not produce any kinematic effect. This could be due to the fact that at this point in time the subject is in the double support period and thus in a more stable position.

A statistical analysis was done across all subjects to confirm the hypothesis that the perturbations significantly change the gait cycle duration. Per subject the mean non-perturbed gait cycle duration was normalized to 100% and the mean perturbed gait cycle duration, for each of the different perturbation conditions, was computed as a percentage with respect to the non-perturbed gait cycle duration, Table I. Forward perturbations produced longer gait cycles, whereas backward perturbations produced shorter gait cycles. A t-test was performed comparing the perturbed and non-perturbed gait cycle durations. Table II shows the p-values for a lower tail t-test where the alternative hypothesis was that the perturbed gait cycle duration was greater than the non-perturbed gait cycle duration (i.e., $P_{\%}$

$> NP_{\%}$). An upper tail t-test was also performed for the opposite case (i.e., $P_{\%} < NP_{\%}$). The backward perturbation conditions (i.e., 100 BWD and 250 BWD) produced a statistically significant shorter duration whereas the forward perturbation conditions (i.e., 100 FWD and 250 FWD) produced a statistically significant greater duration. This shows that overall the perturbations where able to advance or delay the gait cycle.

A cross-correlation analysis can measure the lag of one time series relative to another [41]. This analysis permits computing the time difference in each joint's kinematic pattern produced by the perturbation [42]. The cross-correlation was taken between the across-subject averaged perturbed and non-perturbed kinematic variables (i.e., hip, knee, and ankle angles) 100 ms after the perturbation occurred, Figure 10. In Table III it can be seen that a backward perturbation produces a positive time shift whereas a forward perturbation produces a negative time shift, which corresponds to our hypothesis. The correlation coefficient was computed between the non-perturbed and perturbed joint trajectories after shifting the perturbed joint trajectories by the time difference computed from the cross-correlation function, Table IV. Correlation coefficients as high as one and as low as 0.96 suggest that 100 ms after the perturbation the joint trajectories remained on their nominal orbit. Furthermore, the phase portrait of each joint angle of the perturbed leg are shown across different perturbations in Figure 12. This representation is useful to see how the joint angles and velocities return to their nominal periodic orbit after the perturbation ends.

IV. DISCUSSION

These results confirm that the proposed mechanism and protocol produced phase shifts in the gait cycle. From Figure 11 it can be seen that a forward perturbation produced a negative time shift whereas a backward perturbation produced a positive time shift. Because the perturbed and nominal trajectories overlap modulo this time shift, we can conclude that the perturbation was along the nominal periodic orbit and thus corresponds to a clean phase shift. Table III shows that the time shift depended on both the direction type (backward or forward) and onset time (100 ms or 250 ms) of the perturbation. For example, a backward perturbation occurring at 100 ms after IC produced half the time shift of a backward perturbation occurring at 250 ms after IC. A similar behavior can be seen from the forward perturbations, this could be related to the stability of the center of mass (COM) of the subject and its sensitivity to accelerations or decelerations of the stance foot at the moment when the perturbation occurred. However, the phase shift was consistent within each timing condition as quantified in Tables I and III.

The phase shifts were congruent between joints except the ankle. In Table III it can be seen that the hip and knee joint kinematics appear synchronized for the remainder of the gait cycle. The ankle joint appears to have a slightly different timing than the other joints after the perturbation. In addition, Figure 12 shows how the joint kinematics return to their nominal periodic orbit after a perturbation. In particular, for the hip and knee joint trajectories it takes about 100 ms from the end of a perturbation to converge back to their nominal periodic orbit whereas for the ankle trajectory it takes longer. One explanation could be that the ankle trajectory was perturbed off its nominal orbit, causing a longer transient effect. There could also be neuromechanical differences between the ankle joint

and the more proximal leg joints. In particular, it seems that the ankle joint is more sensitive to the perturbation. Similar conclusions were reached in [43] and [6], where a proximo-distal control is hypothesized in biped locomotion. In this hypothesis the most distal joint (i.e., ankle joint) is influenced by a force feedback loop during locomotion, whereas the more proximal joints (i.e., hip and knee joints) are ruled by feedforward control from the spinal cord.

Due to the fact that the trials were randomized it was impossible for the subject to compensate in any particular direction, but it was possible to co-contract their muscles in order to stiffen their leg. The EMG signals suggest that the majority of the subjects did not anticipate or compensate the perturbation. Upon visual inspection, abnormal co-contractions may have occurred at the beginning (0% – 5%) and end (95% – 100%) of the gait cycle, but not during the time when a perturbation could have occurred, Figure 13. Subjects quickly felt comfortable with the procedure after experiencing the first set of perturbations.

The data gathered from these experiments will be publicly available for scientists (see supplemental downloadable dataset) to use in simulations and tests of neuromechanical hypotheses. As previously mentioned in the introduction, there are multiple hypotheses about the neuromechanics involved during locomotion. Due to the simplicity of the perturbation used in these experiments, scientists could simulate a perturbation of the same magnitude and response time as the one presented here and apply it to their models, e.g., [12] and [17]. One could compare the response of their models with respect to the actual human response, and thus help evaluate and improve their models.

These results also demonstrate that this perturbation mechanism is appropriately designed to study the phase variable hypothesis (i.e., whether a single mechanical variable is capable of parameterizing the gait cycle of a human). The mechanism was able to perturb the joint angles during the stance period of the gait cycle at specific times. Tables I and II show that perturbations caused a phase shift in the kinematics (Figure 11) by accelerating or slowing the gait cycle as hypothesized. Therefore, this mechanism can be used to investigate the potential relationship between the joint kinematic responses and phase variable candidates [6].

V. CONCLUSION

This paper presented the design and validation of a perturbation mechanism and an experimental protocol capable of producing clean phase-shifting perturbations during the gait cycle. During experiments, the perturbation mechanism moved the stance foot 5 cm in a time span of 100 ms. The experimental protocol was validated by statistically analyzing the time shifts and correlations of the joint angle trajectories between perturbed and non-perturbed conditions. The perturbed joint kinematics did not deviate substantially from their nominal periodic trajectories, thus demonstrating a clean shift of the gait cycle phase. The kinematic, kinetic, and EMG data from this paper will allow scientists to test various neuromechanical hypotheses regarding the synchronization of the joints and coordination of the legs during human locomotion.

Supplementary Material

Refer to Web version on PubMed Central for supplementary material.

Acknowledgments

The authors would like to thank Adrian Aleman for his help analyzing the EMG signals.

Robert D. Gregg, IV, Ph.D., holds a Career Award at the Scientific Interface from the Burroughs Wellcome Fund. This work was also supported by the Eunice Kennedy Shriver National Institute of Child Health & Human Development of the National Institutes of Health under Award Number DP2HD080349. The content is solely the responsibility of the authors and does not necessarily represent the official views of the NIH. Dario J. Villarreal holds a Graduate Fellowship from the National Council of Science and Technology (CONACYT) from Mexico.

References

1. Clarac F. Some historical reflections on the neural control of locomotion. Brain research reviews. Jan; 2008 57(1):13–21. [Online]. Available: http://www.ncbi.nlm.nih.gov/pubmed/17919733. [PubMed: 17919733]
2. Haynes C, Lockhart TE. Evaluation of gait and slip parameters for adults with intellectual disability. Journal of Biomechanics. Sep; 2012 45(14):2337–41. [PubMed: 22867766]
3. Pai Y-C, Bhatt TS. Repeated-Slip Training: An Emerging Paradigm for Prevention of Slip-Related Falls Among Older Adults. Physical Therapy. Nov; 2007 87(11):1478–1491. [Online]. Available: http://ptjournal.apta.org/cgi/doi/10.2522/ptj.20060326. [PubMed: 17712033]
4. Parijat P, Lockhart TE. Effects of moveable platform training in preventing slip-induced falls in older adults. Annals of Biomedical Engineering. May; 2012 40(5):1111–21. [PubMed: 22134467]
5. Gregg, RD.; Sensinger, JW. Amer Control Conf. Washington, DC: 2013. Biomimetic virtual constraint control of a transfemoral powered prosthetic leg; p. 5702-5708.
6. Villarreal DJ, Poonawala H, Gregg RD. A robust parameterization of human joint patterns across phase-shifting perturbations. IEEE Transactions on Neural Systems & Rehabilitation Engineering. 2016 conditionally accepted.
7. Grizzle, J.; Westervelt, E.; Chevallereau, C.; Choi, J.; Morris, B. Feedback Control of Dynamic Bipedal Robot Locomotion. Boca Raton, FL: CRC Press; 2007.
8. Sreenath K, Park H-W, Poulakakis I, Grizzle JW. A compliant Hybrid Zero Dynamics controller for stable, efficient and fast bipedal walking on MABEL. The International Journal of Robotics Research. Sep; 2010 30(9):1170–1193.
9. Ramezani A, Hurst JW, Akbari Hamed K, Grizzle JW. Performance analysis and feedback control of ATRIAS, a three-dimensional bipedal robot. ASME Journal of Dynamic Systems, Measurement, and Control. Dec.2013 136(2):021012.
10. Buss BG, Ramezani A, Hamed KA, Griffin BA, Galloway KS, Grizzle JW. Preliminary Walking Experiments with Underactuated 3D Bipedal Robot MARLO. IEEE International Conference on Intelligent Robots and Systems. 2014
11. Hamed KA, Grizzle JW. Event-Based Stabilization of Periodic Orbits for Underactuated 3-D Bipedal Robots With Left-Right Symmetry. IEEE Transactions on Robotics. Apr; 2014 30(2):365–381. [Online]. Available: http://ieeexplore.ieee.org/lpdocs/epic03/wrapper.htm?arnumber=6663683.
12. Dzeladini F, Van Den Kieboom J, Ijspeert A. The contribution of a central pattern generator in a reflex-based neuromuscular model. Frontiers in Human Neuroscience. 2014; 8(371)
13. Rybak IA, Shevtsova NA, Lafreniere-Roula M, McCrea DA. Modelling spinal circuitry involved in locomotor pattern generation: insights from deletions during fictive locomotion. The Journal of Physiology. Dec; 2006 577(Pt 2):617–39. [Online]. Available: http://www.pubmedcentral.nih.gov/articlerender.fcgi?artid=1890439\&tool=pmcentrez\&rendertype=abstract. [PubMed: 17008376]
14. Vogelstein RJ, Etienne-Cummings R, Thakor NV, Cohen AH. Phase-dependent effects of spinal cord stimulation on locomotor activity. IEEE Transactions on Neural Systems and Rehabilitation Engineering. Sep; 2006 14(3):257–65. [PubMed: 17009484]

15. Taghvaei A, Hutchinson SA, Mehta PG. A coupled oscillators-based control architecture for locomotory gaits. 53rd IEEE Conference on Decision and Control. 2014:3487–3492.
16. Tilton AK, Hsiao-Wecksler ET, Mehta PG. Filtering with rhythms: Application to estimation of gait cycle. American Control Conference. 2012:3433–3438.
17. Song S, Geyer H. A neural circuitry that emphasizes spinal feedback generates diverse behaviours of human locomotion. The Journal of Physiology. Aug; 2015 593(16):3493–3511. [Online]. Available: http://doi.wiley.com/10.1113/JP270228. [PubMed: 25920414]
18. Prochazka A, Yakovenko S. The neuromechanical tuning hypothesis. Progress in Brain Research. 2007; 165:255–265. [PubMed: 17925251]
19. Villarreal DJ, Quintero D, Gregg RD. A perturbation mechanism for investigations of phase variables behavior in human locomotion. IEEE International Conference on Robotics and Biomimetics. 2015
20. Keesman, KJ. System Identification An Introduction. New York: Springer; 2011.
21. Rouse EJ, Hargrove LJ, Perreault EJ, Peshkin M, Kuiken T. Development of a mechatronic platform and validation of methods for estimating ankle stiffness during the stance phase of walking. Journal of Biomechanical Engineering. 2013; 135(8):81009. [PubMed: 23719922]
22. Roy, A.; Krebs, HI.; Patterson, SL.; Judkins, TN.; Khanna, I.; Forrester, LW.; Macko, RM.; Hogan, N. 2007 IEEE 10th International Conference on Rehabilitation Robotics. Vol. 00. IEEE; Jun. 2007 Measurement of Human Ankle Stiffness Using the Anklebot; p. 356-363.[Online]. Available: http://ieeexplore.ieee.org/lpdocs/epic03/wrapper.htm?arnumber=4428450
23. Lee, Hyunglae; Ho, P.; Rastgaar, M.; Krebs, HI.; Hogan, N. Multivariable Static Ankle Mechanical Impedance With Active Muscles. IEEE Transactions on Neural Systems and Rehabilitation Engineering. Jan; 2014 22(1):44–52. [On-line]. Available: http://dx.doi.org/10.1016/j.jbiomech.2011.04.028http://ieeexplore.ieee.org/lpdocs/epic03/wrapper.htm?arnumber=6605642. [PubMed: 24107970]
24. Lee H, Hogan N. Time-Varying Ankle Mechanical Impedance During Human Locomotion. IEEE transactions on neural systems and rehabilitation engineering: a publication of the IEEE Engineering in Medicine and Biology Society. 2014; 4320(c):755–764. [Online]. Available: http://www.ncbi.nlm.nih.gov/pubmed/25137730.
25. Tucker, MR.; Moser, A.; Lambercy, O.; Sulzer, J.; Gassert, R. 2013 IEEE 13th International Conference on Rehabilitation Robotics (ICORR). IEEE; Jun. 2013 Design of a wearable perturbator for human knee impedance estimation during gait; p. 1-6.[Online]. Available: http://ieeexplore.ieee.org/lpdocs/epic03/wrapper.htm?arnumber=6650372
26. Gregg RD, Rouse EJ, Hargrove LJ, Sensinger JW. Evidence for a time-invariant phase variable in human ankle control. PLoS ONE. Jan.2014 9(2):e89163. [PubMed: 24558485]
27. van Doornik J, Sinkjaer T. Robotic platform for human gait analysis. IEEE Transactions on Biomedical Engineering. 2007; 54(9):1696–1702. [PubMed: 17867362]
28. Tang PF, Woollacott MH, Chong RKY. Control of reactive balance adjustments in perturbed human walking: Roles of proximal and distal postural muscle activity. Experimental Brain Research. 1998; 119(2):141–152. [PubMed: 9535563]
29. Dietz V, Horstmann GA, Berger W. Interlimb coordination of leg-muscle activation during perturbation of stance in humans. Journal of Neurophysiology. Sep; 1989 62(3):680–93. [Online]. Available: http://www.ncbi.nlm.nih.gov/pubmed/2769353. [PubMed: 2769353]
30. Trkov M, Yi J, Liu T, Li K. Shoe-floor interactions during human slip and fall: Modeling and experiments. ASME Dynamic Systems and Control Conference. 2014
31. Handzic, I.; Reed, KB. 2013 IEEE 13th International Conference on Rehabilitation Robotics (ICORR). Vol. 2013. IEEE; Jun. 2013 Comparison of the passive dynamics of walking on ground, tied-belt and split-belt treadmills, and via the Gait Enhancing Mobile Shoe (GEMS); p. 1-6.[On-line]. Available: http://dx.doi.org/10.1109/ICORR.2013.6650509http://ieeexplore.ieee.org/lpdocs/epic03/wrapper.htm?arnumber=6650509
32. Handzic, I.; Vasudevan, E.; Reed, KB. Developing a Gait Enhancing Mobile Shoe to alter over-ground walking coordination; 2012 IEEE International Conference on Robotics and Automation IEEE. May. 2012 p. 4124-4129.[Online]. Available: http://ieeexplore.ieee.org/lpdocs/epic03/wrapper.htm?arnumber=6225346

33. Logan D, Ivanenko YP, Kiemel T, Cappellini G, Sylos-Labini F, Lacquaniti F, Jeka JJ. Function dictates the phase dependence of vision during human locomotion. Journal of Neurophysiology. 2014
34. Owings TM, Pavol MJ, Grabiner MD. Mechanisms of failed recovery following postural perturbations on a motorized treadmill mimic those associated with an actual forward trip. Clinical Biomechanics. Nov; 2001 16(9):813–819. [Online]. Available: http://linkinghub.elsevier.com/retrieve/pii/S0268003301000778. [PubMed: 11714559]
35. Dietz V, Quintern J, Sillem M. Stumbling reactions in man: significance of proprioceptive and pre-programmed mechanisms. The Journal of Physiology. May; 1987 386(1):149–163. [Online]. Available: http://doi.wiley.com/10.1113/jphysiol.1987.sp016527. [PubMed: 3681704]
36. Vilensky JA, Cook JA, Cooper JL. Stumbling corrective responses in healthy human subjects to rapid reversal of treadmill direction. Journal of Electromyography and Kinesiology. Apr; 1999 9(3):161–171. [On-line]. Available: http://www.ncbi.nlm.nih.gov/pubmed/10328411http://linkinghub.elsevier.com/retrieve/pii/S1050641198000273. [PubMed: 10328411]
37. Villarreal DJ, Gregg RD. A survey of phase variable candidates of human locomotion. IEEE Engineering in Medicine and Biology Conf. 2014:4017–21.
38. Grabiner MD, Feuerbach JW, Lundin TM, Davis BL. Visual guidance to force plates does not influence ground reaction force variability. Journal of Biomechanics. 1995; 28(9):1115–7. [PubMed: 7559681]
39. Verniba D, Vergara ME, Gage WH. Force plate targeting has no effect on spatiotemporal gait measures and their variability in young and healthy population. Gait & Posture. Feb; 2015 41(2): 551–556. [Online]. Available: http://linkinghub.elsevier.com/retrieve/pii/S096663621400798X. [PubMed: 25737237]
40. Konrad, P. The ABC of EMG. Scottsdale, AZ: Noraxon; 2006.
41. Proakis, JG.; Manolakis, DK. Digital Signal Processing. 4th. New Jersey, USA: Prentice Hall; 2006.
42. Winter, D. Biomechancis and Motor Control of Human Movement. Wiley, J.; Inc, S., editors. Hoboken, NJ: 2009.
43. Daley MA, Felix G, Biewener AA. Running stability is enhanced by a proximo-distal gradient in joint neuromechanical control. The Journal of Experimental Biology. 2007; 210:383–394. [PubMed: 17234607]

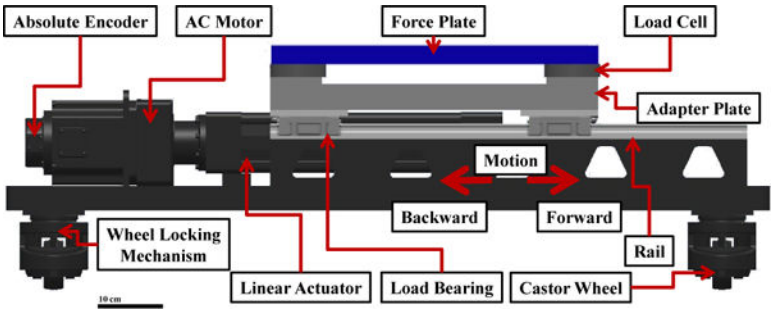

Fig. 1.

Schematic diagram of the translational perturbation mechanism with highlighted features. The force plate on top of the mechanism is able to measure the GRF of the subject.

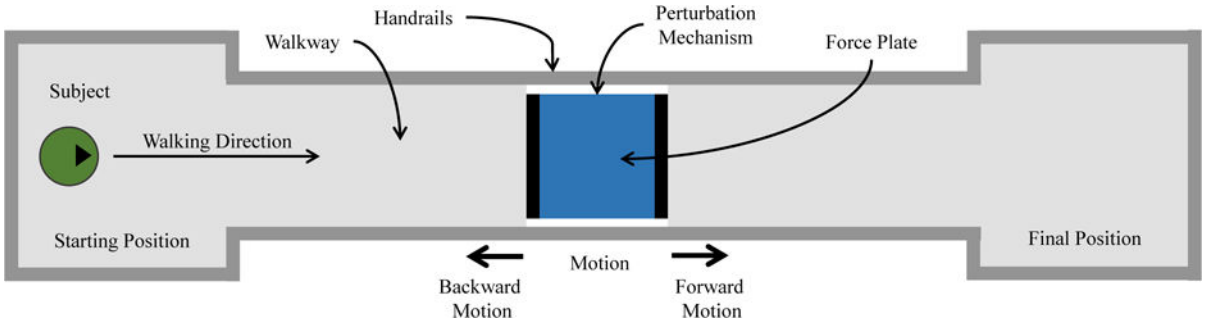

Fig. 2.

Top view of the experimental setup. The subject walked along an 8 m walkway, stepping on the force plate in the center. The perturbation mechanism produced a perturbation at random when the subject stepped on it. The subject was asked to walk naturally from the starting position to the final position, after which the subject turned around and repeated.

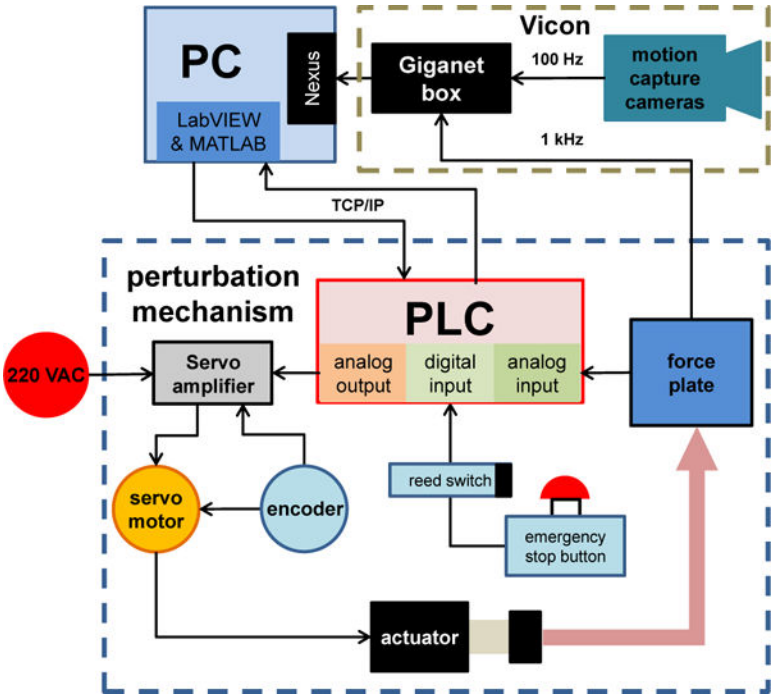

Fig. 3.

Connection diagram of the perturbation mechanism with highlighted hardware. The perturbation mechanism reads the analog signal from the force plate to later actuate the platform through a servomotor. The motion capture cameras and Giganet box acquire and synchronize the experimental data to be stored and post-processed in a PC.

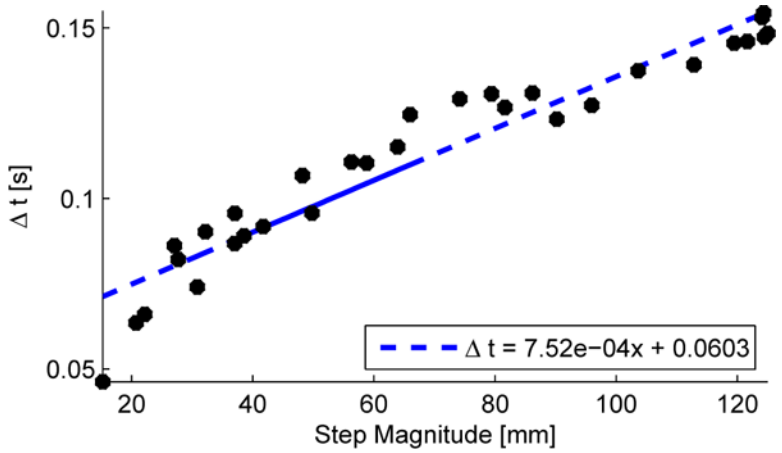

Fig. 4.

The magnitude of a perturbation (x-axis) versus the time needed to achieve such magnitude. ($r^2 = 0.92$).

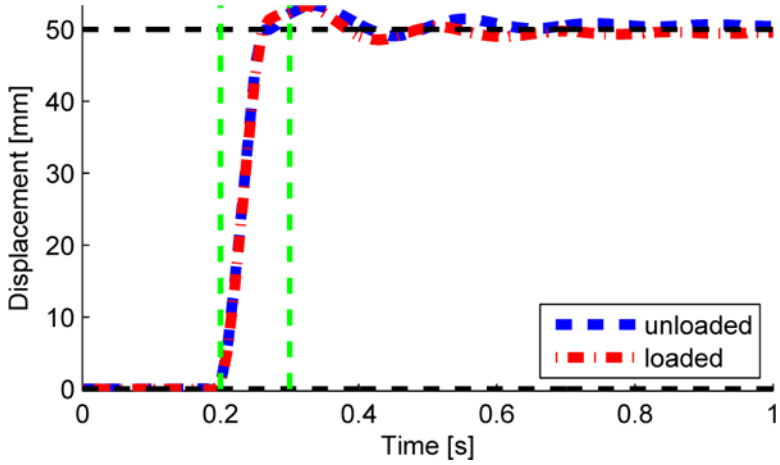

Fig. 5.

Motion of the perturbation unloaded (blue dashed line) and loaded (red dash-dot line) in the forward direction. Green dashed vertical lines show the time span of the perturbation, roughly 100 ms. Black dashed horizontal lines are the initial and final desired values of the perturbation.

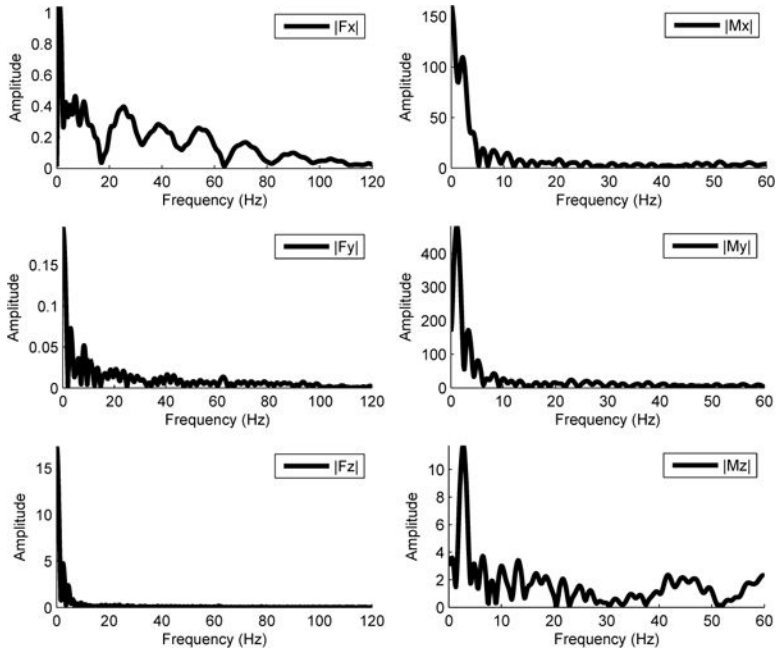

Fig. 6.

Frequency analysis of the raw forces and moments signals collected from the loaded force plate. Fx, Fy, and Fz are the forces in the x, y, and z axes, respectively. Mx, My, and Mz are the moments in the x, y, and z axes, respectively.

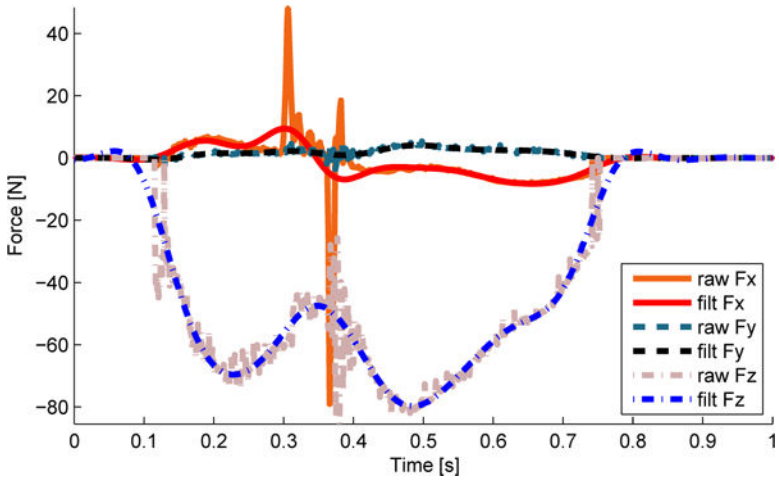

Fig. 7.

Comparison between raw and filtered (filt) forces and moments collected from the loaded force plate. Fx, Fy, and Fz are the forces in the x, y, and z axes, respectively.

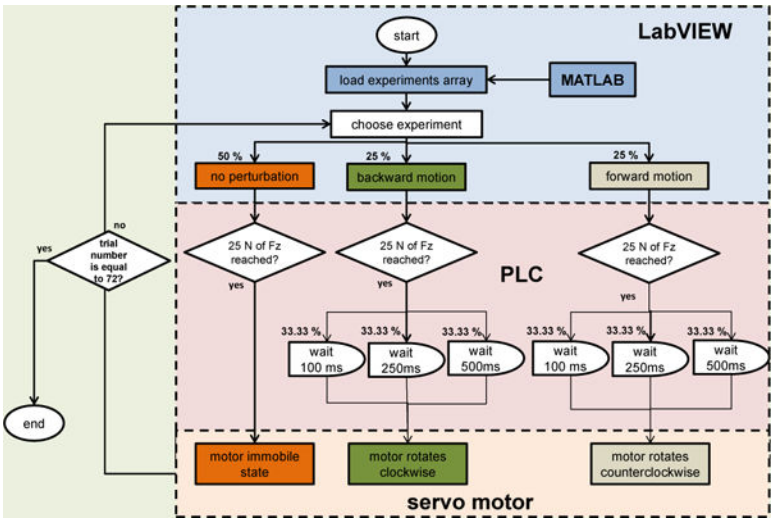

Fig. 8.

Flow diagram of the algorithm used to control the perturbation mechanism across all trials. The percentages represent the probability of incidence of each experiment across all trials.

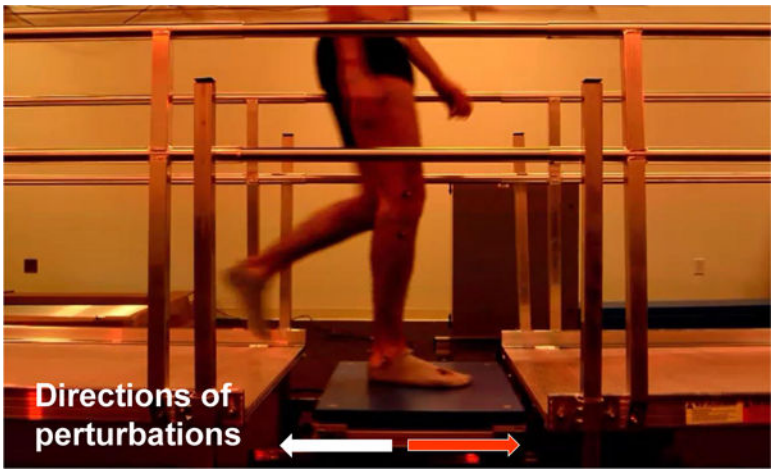

Fig. 9.
Picture of a subject during a perturbation trial.

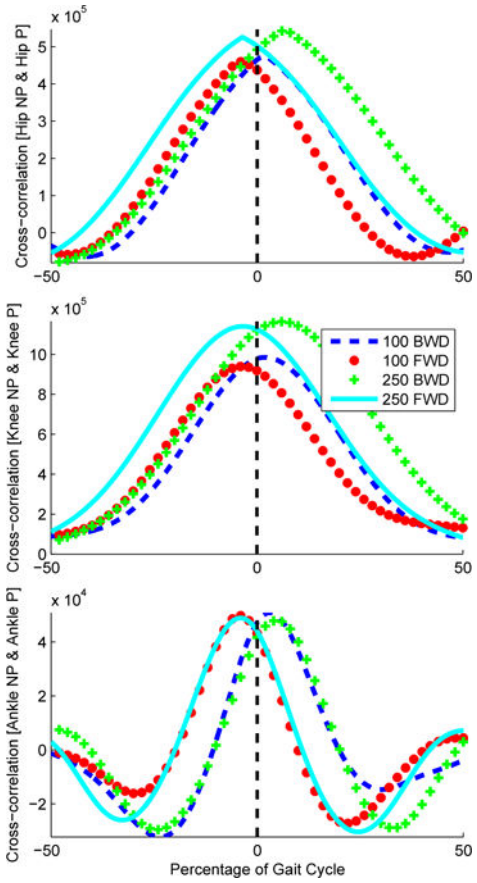

Fig. 10.

Results from the cross-correlation function across each joint angle trajectory, i.e., hip (top), knee (middle), and ankle (bottom). “NP” stands for non-perturbed trajectories whereas “P” stands for perturbed trajectories. The lag of the signals is normalized by the percentage of the gait cycle.

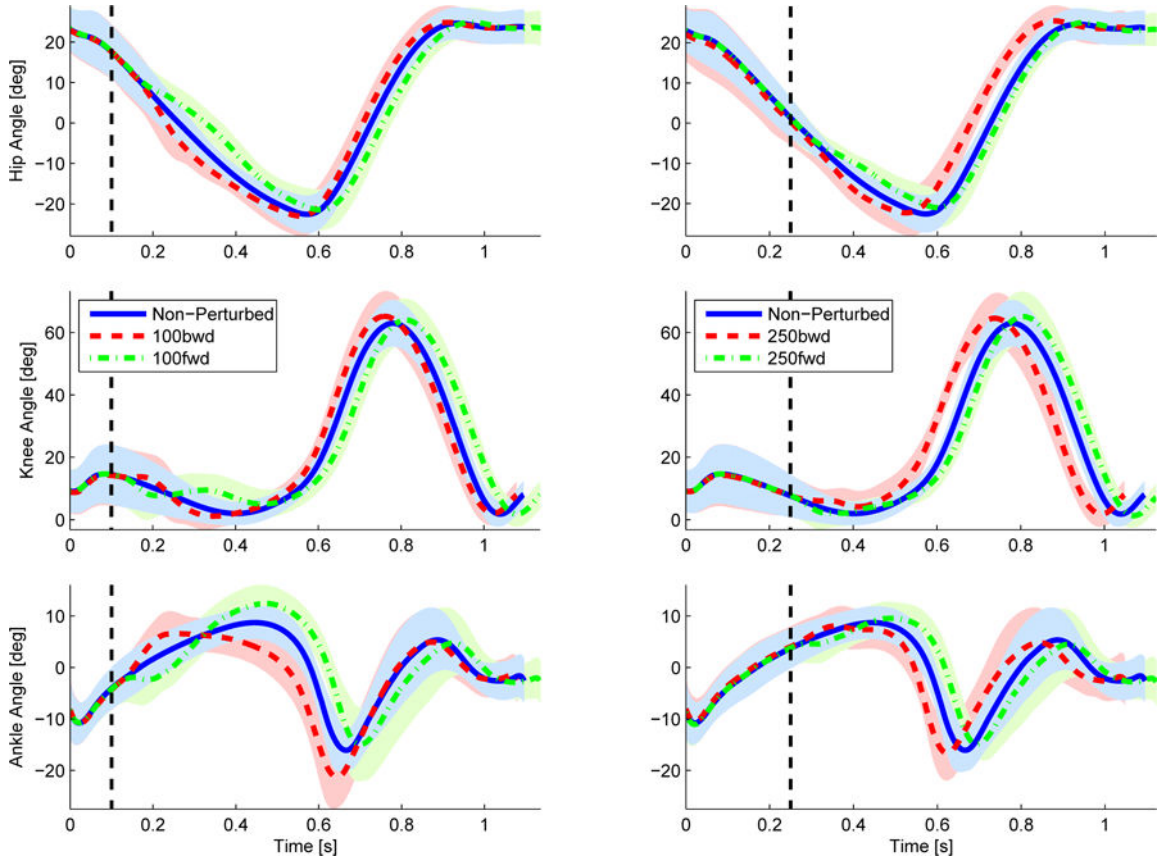

Fig. 11.

Hip, knee, and ankle angles of the initiating leg (i.e., leg stepping on the force plate) over time with and without perturbations occurring at 100 ms (left) and 250 ms (right) after IC. The shaded region represents one standard deviation away from the mean.

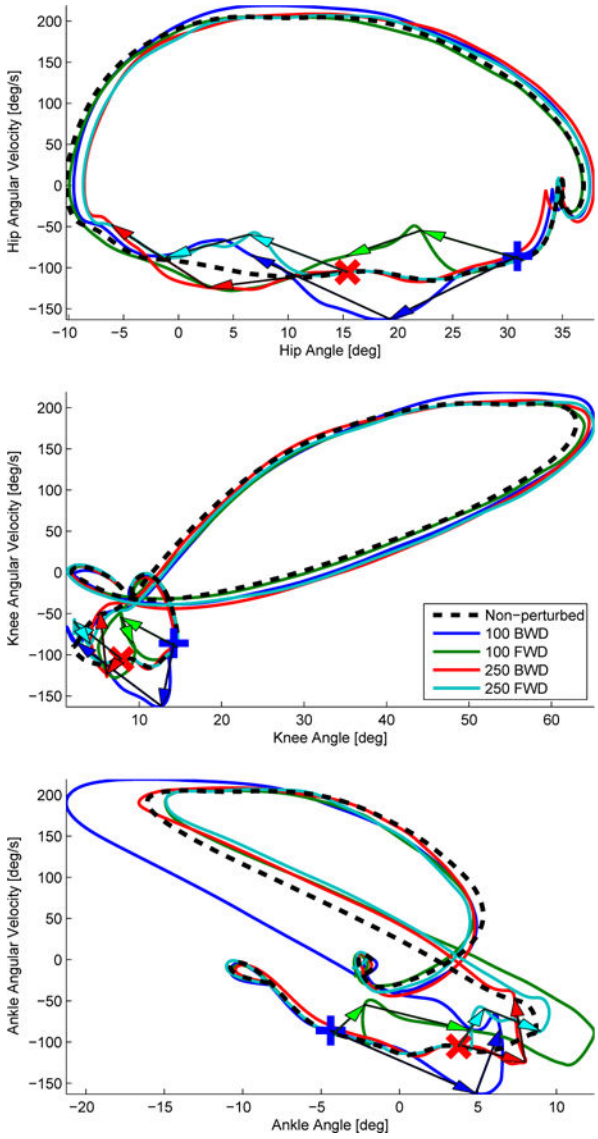

Fig. 12.

Phase portraits across different perturbation conditions of the perturbed leg joint angle trajectories: hip (top), knee (middle), and ankle (bottom). The length of each arrow represents a 100 ms time difference between the origin and the head of the arrow. The head of the arrow is pointing towards the motion of the phase portrait. Note that the second arrows (representing 200 ms after perturbation onset) point approximately back to the nominal orbits. The blue plus sign and red cross sign represent the 100 ms and 250 ms perturbation onset times after initial contact, respectively.

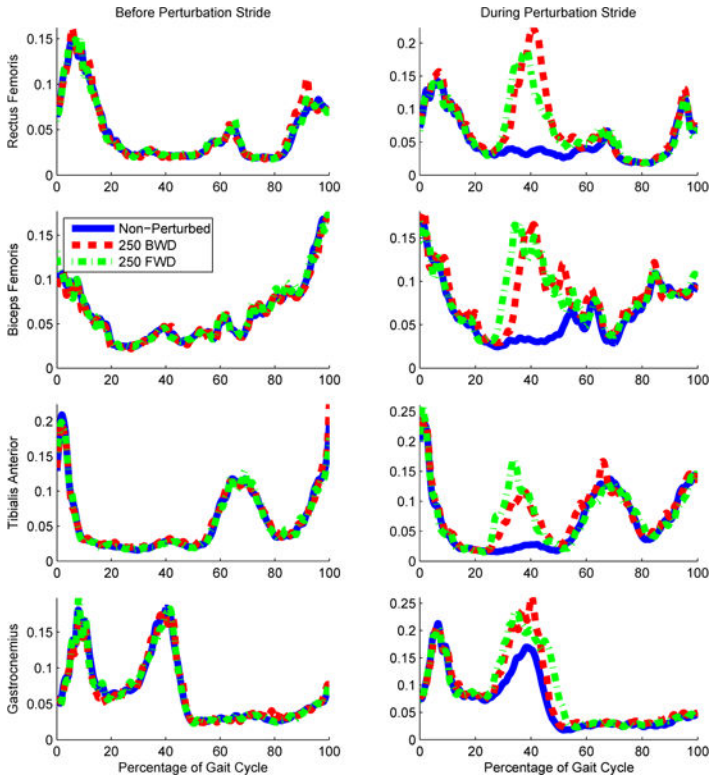

Fig. 13.

The averaged normalized EMG signals across subjects for the rectus femoris, biceps femoris, tibialis anterior, and gasctrocnemius muscles are shown for the gait cycle prior to stepping on the perturbation platform (left column) and the gait cycle starting with a step on the perturbation platform (right column). Time is normalized to percentage of the gait cycle in order to show the differences between activations during each perturbation condition (i.e., nominal condition and a forward and a backward perturbation 250 ms after initial contact with the force plate).

TABLE I

Normalized duration of perturbed gait cycles with respect to non-perturbed gait cycles

Subject	100 BWD	100 FWD	250 BWD	250 FWD
1	99.829	107.358	99.440	107.867
2	97.281	100.307	96.698	101.405
3	98.619	104.519	97.354	101.742
4	97.532	101.063	93.002	101.097
5	98.627	101.450	98.532	101.909
6	97.422	103.213	98.492	99.823
7	98.989	105.367	96.379	102.223
8	100.001	103.957	95.681	101.845
9	97.634	102.237	94.762	100.509
10	97.625	105.461	85.664	105.005
Mean	98.356	103.493	95.600	102.343
STD	0.958	2.132	3.779	2.249

Mean duration of the gait cycle (in percentage with respect to the mean non-perturbed gait cycle duration) for each subject across multiple types of perturbations.

TABLE II

P-values for the comparison between perturbed and non-perturbed gait cycle duration

	100 BWD	100 FWD	250 BWD	250 FWD
$P_{\%} < NP_{\%}$	<<0.05	1.000	<<0.05	0.997
$P_{\%} > NP_{\%}$	1.000	<<0.05	0.999	<<0.05

The p-values are shown for the comparison between the time duration (in percentage of the gait cycle) of perturbed and non-perturbed gait cycles across different types of perturbations. The null hypothesis is defined as $P_{\%} = NP_{\%}$ which means that the percentage change produced by a perturbation is zero. $P_{\%} < NP_{\%}$ represents the alternative hypothesis that the perturbed gait cycle was shorter than the non-perturbed gait cycle, whereas $P_{\%} > NP_{\%}$ represents the opposite alternative hypothesis.

TABLE III

Gait cycle time shift produced by the perturbation

	100BWD	100FWD	250BWD	250FWD
Hip	0.0170	−0.0384	0.0485	−0.0263
Knee	0.0170	−0.0328	0.0455	−0.0255
Ankle	0.0278	−0.0374	0.0350	−0.0294
Mean (s)	0.0206	−0.0362	0.0430	−0.0271

TABLE IV

Correlation Coefficients between Non-perturbed and Perturbed joint trajectories after time shift

Perturbation	Hip	Knee	Ankle
100BWD	0.999	0.999	0.960
100FWD	0.999	0.997	0.981
250BWD	1.000	0.999	0.998
250FWD	1.000	1.000	0.992
Mean	0.999	0.999	0.983
STD	0.000	0.001	0.017

The correlation coefficients were computed after shifting the perturbed joint trajectories by the time difference computed from the cross-correlation, Table III.